

# Real-Time Video Inference on Edge Devices via Adaptive Model Streaming

Mehrdad Khani, Pouya Hamadanian, Arash Nasr-Esfahany, Mohammad Alizadeh

MIT CSAIL

{khani,pouyah,arashne,alizadeh}@csail.mit.edu

## Abstract

Real-time video inference on compute-limited edge devices like mobile phones and drones is challenging due to the high computation cost of Deep Neural Network models. In this paper we propose Adaptive Model Streaming (AMS), a cloud-assisted approach to real-time video inference on edge devices. The key idea in AMS is to use online learning to continually adapt a lightweight model running on an edge device to boost its performance on the video scenes in real-time. The model is trained in a cloud server and is periodically sent to the edge device. We discuss the challenges of online learning for video and present a practical design that takes into account the edge device, cloud server, and network bandwidth resource limitations. On the task of video semantic segmentation, our experimental results show 5.1–17.0 percent mean Intersection-over-Union improvement compared to a pre-trained model on several real-world videos. Our prototype can perform video segmentation at 30 frames-per-second with 40 milliseconds camera-to-label latency on a Samsung Galaxy S10+ mobile phone, using less than 400Kbps uplink and downlink bandwidth on the device.

## 1 Introduction

Real-time video inference is a core component for a wide range of applications, such as augmented reality, drone-based sensing, robotic vision, and autonomous driving. These applications use Deep Neural Networks (DNNs) for inference tasks like object detection [1], semantic segmentation [2], and pose estimation [3]. Unfortunately, state-of-the-art DNN models are too expensive to run on low-powered edge devices like mobile phones, drones, and consumer robots. For example, large semantic segmentation and object detection models take several seconds to run on mobile phones [4, 5]. Running such models in real-time is beyond even the capabilities of accelerators such as Coral Edge TPU [6] and NVIDIA Jetson [7] that are compact enough to mount on small drones and robots [8–10].

There are two broad approaches to tackling this problem today. The first is to specialize the DNN models for low-powered devices [11–13]. It is common practice for state-of-the-art models to come with lightweight, mobile-friendly versions that use a smaller backbone neural network. However, using these models typically involves a significant compromise in performance. For example, for semantic segmentation, models like DeeplabV3 [2] with Xception65 [14] backbone have surpassed a mean Intersection-over-Union (mIoU) [15] of 82% on the Cityscapes dataset [16], but a lightweight model based on the MobileNetV2 [11] backbone can only achieve an mIoU of 70% [4]. This large gap in performance is also seen in other complex tasks like object detection [17, 12]. The second approach is to offload inference to a powerful remote machine [18–20]. Remote inference requires a high network bandwidth to stream the entire video to the remote machine, and each frame incurs a delay (e.g., 100s of milliseconds) to pass through the video-encoder and the network, making it hard to meet the tight latency requirements of some applications [21]. Moreover, remote inference techniques are susceptible to network outages, which are a common occurrence on wireless networks [22]. Proposals

like edge computing [23–25] that place the remote machine close to the edge devices lessen these barriers, but do not eliminate them and incur additional infrastructure and maintenance costs.

In this paper we propose *Adaptive Model Streaming* (AMS), a new design paradigm for real-time video inference on edge devices. AMS uses a remote server to *continually adapt* a lightweight model running on the edge device to boost its accuracy for the particular video in real time. The edge device sends sample video frames to the remote server, which uses them to fine-tune a copy of the edge device’s model to mimic a large, expensive model via supervised knowledge distillation [26]. The server periodically sends (or “streams”) the updated lightweight model to the edge device for inference. The insight underlying AMS is that lightweight models perform poorly because they lack the capacity to learn an accurate model over a wide variety of video frames. By exploiting the temporal locality in video frames and adapting the model frequently (e.g., every 10 seconds), AMS overcomes the challenges associated with the low capacity of mobile-friendly models. AMS also avoids the drawbacks of remote inference approaches. It requires much less bandwidth to send training samples to the server (e.g., one frame per second) than to send the entire video, and network delay or outages do not affect the inference latency since inference takes place locally on the device.

We present a design that addresses two main challenges with realizing AMS in practice. First, in order for AMS to respond to the changes in the video quickly, we need fast adaptation algorithms at the server. We use a simple online gradient descent approach that continually adapts the model at the server based on recent samples from a suitably chosen time horizon. Second, we develop techniques to reduce the downlink and uplink bandwidth requirements for AMS. In the downlink, naively streaming a small semantic segmentation model with 2 million (float16) parameters every 10 seconds would require over 3 Mbps of bandwidth. Our design uses coordinate descent [27, 28] to train and send a small fraction of the model parameters in each update. We show that dynamically selecting 5% of the parameters to send based on gradient signals reduces the downlink bandwidth to only 230 Kbps with negligible loss in performance. In the uplink, we use standard H.264 video encoding [29] to compress and upload the training samples to the server every few seconds, requiring a modest 100–400 Kbps. To put AMS’s bandwidth requirement in perspective, it is less than the YouTube recommended bitrate range of 300–700 Kbps to live stream video at the lowest 240p resolution [30].

We evaluate our approach for real-time semantic segmentation on a Samsung Galaxy S10+ phone (with Adreno 640 GPU) using 7 real-world videos that span a variety of outdoor scenarios, including fixed cameras and moving cameras at walking, running, and driving speeds. Compared to a lightweight model (DeeplabV3 with MobileNetV2 [11] backbone) pretrained on the Cityscapes dataset [16] without video-specific customization, AMS provides a 5.1–17.0% boost (10.8% on average) in mIoU metric (computed relative to the labels from a state-of-the-art DeeplabV3 with Xception65 [14] backbone model) depending on the video. Also, compared to an approach that customized the model once for each video based on the first 60 seconds, AMS improves mIoU by 0.1–15.5% (6.5% on average). Figure 1 shows four visual examples comparing the performance of these on-device approaches to a large, state-of-the-art model. We will release our code and video datasets at <https://github.com/modelstreaming/ams>.

## 2 Related Work

**Real-time On-Device Inference.** Lightweight mobile-friendly models have been designed both manually [11] and using neural architecture search techniques [31, 32]. Model quantization and weight pruning techniques [33–36] have further been shown to reduce the computation footprint of such models with a small loss in accuracy. Specific to video, some techniques amortize the inference cost by using optical flow methods to skip inference for some frames [37–39]. Despite the significant progress made with these optimization techniques, there remains a large gap in the performance of lightweight models and state-of-the-art solutions. AMS is complementary to on-device optimization techniques and would also benefit from them. Several proposals offload all or part of the computation to a powerful remote machine [40–42, 18–20], but these schemes generally require high network bandwidth, incur higher latency, and are susceptible to network outages [21, 19].

**Model Adaptation.** Our work is closely related to online learning [43] algorithms for minimizing dynamic or tracking regret [44–46]. Dynamic regret compares the performance of an online learner to a sequence of optimal solutions. In our case, the goal is to track the performance of the best lightweight model at each point in a video. Dynamic regret problems have lower bounds that relate

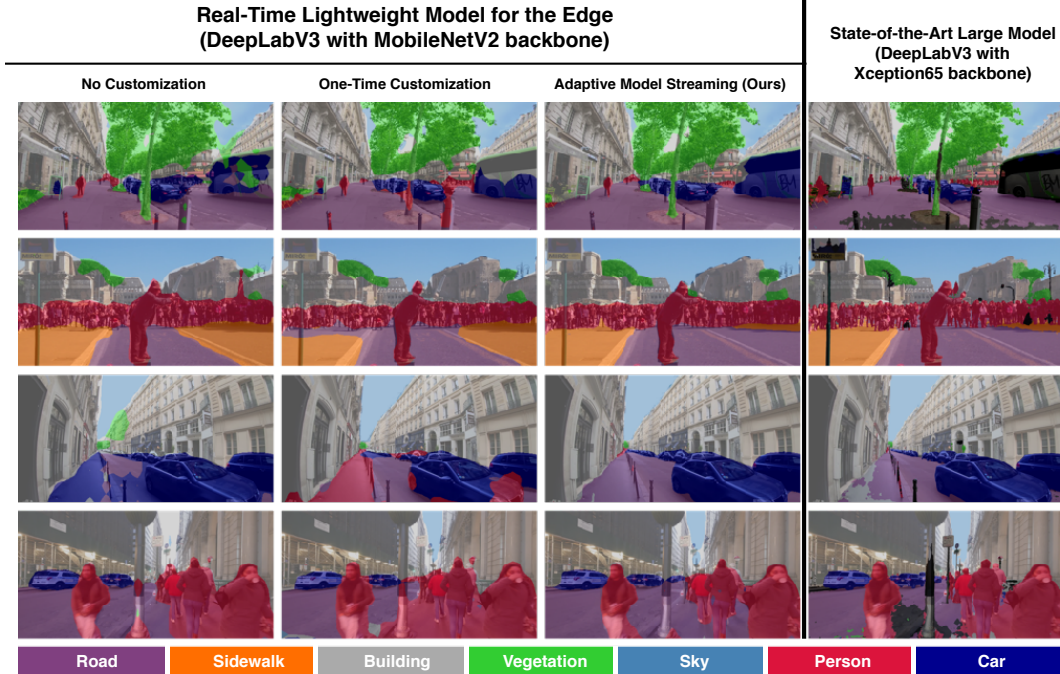


**Figure 1:** Semantic segmentation results on real-world outdoor videos: columns from left to right represent No Customization, One-Time Customization, and AMS. For reference, the results for a large, expensive model are shown in the last column. AMS provides better accuracy and reduces artifacts (e.g., see the sidewalk detected in error by the no/one-time customized models in the second row). Notice that the large model (trained on Cityscapes) also makes some mistakes on these real-world videos. Since AMS aims to mimic the large model via continual knowledge distillation, its accuracy will improve with a better large model.

regret to a measure of complexity of the optimal sequence of decisions, for example, how quickly the best model parameters change with time [44]. As video scenes change slowly, it is plausible that the best models also change gradually in time and online learning can be effective. Several theoretical works have studied online gradient descent algorithms in this setting with different assumptions about the loss functions [47, 48]. Other work has focused on the “experts” setting [49–51], where the learner maintains multiple models and uses the best of them at each time. Our approach is based on online gradient descent because tracking multiple models per video at a server is expensive.

Other paradigms for model adaptation include lifelong/continual learning [52], meta-learning [53, 54], federated learning [55], and unsupervised domain adaptation [56, 57]. As our work is only tangentially related to these efforts, we defer their discussion to Appendix B.

**Distillation for Video.** Distillation [26] has been proposed as a way to accelerate video inference for a large corpus of videos [58, 59]. Noscope [58] trains small models for specific tasks (e.g., detecting a few object classes) on specific videos offline. JITNet [59] uses online distillation to specialize a model on video frames as they arrive. The key difference between these works and ours is that they perform training and inference on the same machine (e.g., server GPU) and the goal is to speed up inference, whereas in AMS, the student model runs at a low-powered edge device in real time, but it is trained online at a remote server with sufficient compute power. In particular, AMS is constrained by limited bandwidth between the edge device and remote server, and crucially uses coordinate-descent-based [27] training for model distillation to significantly reduce bandwidth requirements.

### 3 How Online Adaptation Boosts Performance of Lightweight Models

AMS improves the performance of a lightweight model at an edge device through continual online adaptation. To gain intuition for how online adaptation improves model performance, we discuss a simple illustrative example in this section.

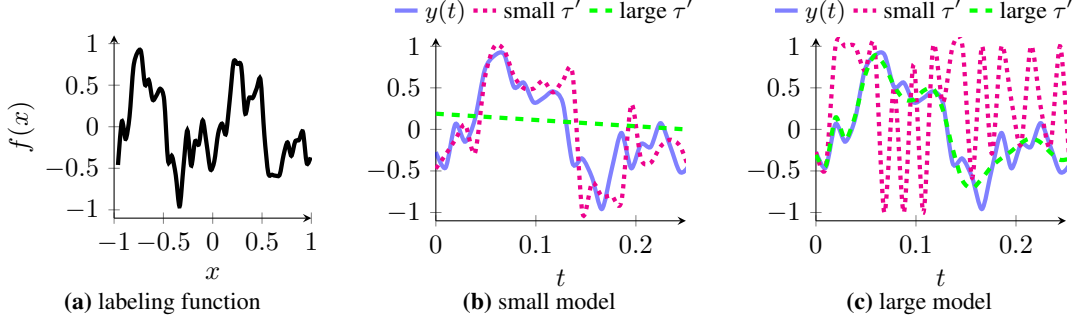


**Figure 2:** A simple example illustrating the importance of considering the model complexity in training horizon.

Let  $\mathcal{X}$  denote the set of possible input values (e.g., frames in a video). We are given a time-varying input sequence  $x(t) \in \mathcal{X}$  and must predict an output  $y(t) \in \mathcal{Y}$  given by a deterministic function of the input:  $y(t) = f(x(t))$ . In video semantic segmentation, for example,  $y(t)$  corresponds to the segmentation of the frame  $x(t)$ . Let us divide time into a sequence of steps of length  $\tau$  seconds. Step  $n$  refers to the time interval  $[n\tau, n\tau + \tau)$ . We refer to  $\tau$  as the *inference horizon*. At the beginning of each step  $n$ , we pick a set of model parameters  $\mathbf{w}_n \in \mathbb{R}^d$  to use for prediction during step  $n$ . As a result, we incur a loss of  $\mathcal{L}_n(\mathbf{w}_n)$ . The goal is to minimize the total loss over time:  $\sum_{n=1}^N \mathcal{L}_n(\mathbf{w}_n)$ .

Consider a scalar regression task where  $\mathcal{X} = \mathcal{Y} = [-1, 1]$ , and the function  $f(\cdot)$  is as shown in Fig. 2a. Suppose  $x(t)$  is a periodic function of time  $t$ , which consists of repeated triangles of unit period, i.e.  $x(t) = 1 - 2|t - 0.5|$  for  $t \in [0, 1]$  defines one period of  $x(t)$ . As time progresses,  $x(t)$  moves back and forth linearly between -1 and 1. Notice that the characteristics of  $f(\cdot)$  change significantly over its domain  $[-1, 1]$ . However, the regression task exhibits temporal locality: since  $x(t)$  changes gradually over time, the regression problem is similar in nearby time intervals. Video inference exhibits a similar temporal locality because the scenes in a video usually change gradually over time.

Suppose we wish to use polynomials of some degree  $d$  to make predictions at each time step. A natural way to exploit temporal locality is to train the model using recent data at each time step. Let us define the *training horizon* as the amount of time into the past used to make a decision and denote it by  $\tau'$ . For step  $n$ , the online learner fits a polynomial of degree  $d$  to  $(x(t), y(t))$  observed over  $t \in [n\tau - \tau', n\tau)$  with Mean-Squared-Error loss, and it uses this model to make predictions in  $t \in [n\tau, n\tau + \tau)$ . We plot  $y(t)$  and its predictions for a small linear model ( $d = 1$ ) and a much larger polynomial model ( $d = 50$ ) in Fig. 2b and Fig. 2c, respectively. For each model, we trained two variants, using small ( $\tau' = 1/64$ ) and large ( $\tau' = 1/2$ ) values for the training horizon. As these plots show, the linear model does not have the capacity to fit the data over a long time horizon. However, by continually adapting the model based on a small training horizon, it is able to make much better predictions. On the other hand, a high-capacity model does not need to be constrained to a short time horizon, and in fact it overfits and has poor accuracy when trained with a small horizon.

This example illustrates the importance of picking a training horizon that is well-matched to the model capacity. Smaller models benefit from a shorter training horizon, i.e. more localized customization over time. We will see that for tasks such as video semantic segmentation, such localized customization of lightweight models can provide a significant boost in accuracy.

## 4 Cloud-Assisted Adaptive Model Streaming for Real-time Video Inference

In this section we describe the design of a practical real-time video inference system that leverages adaptive model streaming. Our goal is to continually adapt a lightweight model for a complex task like video semantic segmentation. Since training on the edge devices is too expensive, we use a cloud server. Each edge device periodically samples video frames and sends them to the cloud server every  $\tau$  seconds. The server uses these frames to train a copy of the edge device’s model using supervised knowledge distillation [26], and sends the updated model to the edge device. Algorithm 1 shows the procedure at the server when it is serving a single edge device (we discuss multiple edge devices in §4.1). The AMS algorithm at the server has two phases: inference and training.

**Inference Phase.** To train, the server first needs to label the incoming video frames. It obtains these labels using a state-of-the-art segmentation model like DeeplabV3 [2] with Xception65 [14] backbone, which is too large to run at the edge. This model acts as a “teacher” for supervised knowledge distillation [26]. As the server receives new sample frames, it runs the teacher model on them to obtain the labels and adds the frames, labels, and frame timestamps to a training data buffer  $\mathcal{B}$ . The training phase uses the labeled frames to train the “student” model that runs on the edge device.

**Training Phase.** As discussed in §3, at the beginning of each step  $n$ , we desire a set of model parameters  $\mathbf{w}_n$  that minimizes the loss of that step  $\mathcal{L}_n(\cdot)$ . The loss  $\mathcal{L}_n(\cdot)$  depends on the *future* video at step  $n$  and is unknown. Therefore we train using the cross-entropy loss over sample frames from the last  $\tau'$  seconds of video. As discussed in §3, choosing a good training horizon directly affects the performance of online adaptation: a large value of  $\tau'$  could make the data distribution too complex for a lightweight model, but too small a  $\tau'$  can also cause the model to overfit. The optimal value of  $\tau'$  depends on the model complexity, and the nature of scene changes in the video (e.g., a fast-changing video may benefit from a shorter  $\tau'$ ). As our results will show, we observed that a training horizon of about three to five minutes works well across a wide range of videos for video semantic segmentation using models based on DeeplabV3 with MobileNetV2 [11] backbone and we set  $\tau'$  to four minutes in our system. To reduce the bandwidth requirement for model streaming (see §4.1), we employ *coordinate descent* [27, 28], in which we train a subset of parameters at each training phase and send only those parameters to the edge device. Specifically, for each training phase, we select a subset of parameter indices,  $\mathcal{I}_n$ , and only update those parameters using the Adam optimizer [60]. We explored several strategies to select  $\mathcal{I}_n$ , as described in detail in §5.3. We found that the *Gradient-Guided* strategy achieves the best accuracy. In this strategy,  $\mathcal{I}_n$  includes the parameters that the optimizer estimates to have the largest impact on the loss function. Appendix C describes this method in detail.

---

**Algorithm 1** *Adaptive Model Streaming (Server)*

---

```

1: Initialize the student model with pre-trained parameters  $\mathbf{w}_0$ 
2: Send  $\mathbf{w}_0$  and the student model architecture for the edge device
3:  $\mathcal{B} \leftarrow$  Initialize a time-stamped buffer to store (sample frame, teacher prediction) tuples
4: for  $n \in \{1, 2, \dots\}$  do
5:   Wait until  $t \geq n\tau$ 
6:    $\mathcal{R}_n \leftarrow$  Set of new sample frames from the edge device  $\triangleright$  Entering Inference Phase
7:   for  $\mathbf{x} \in \mathcal{R}_n$  do
8:      $\tilde{\mathbf{y}} \leftarrow$  Use the teacher model to infer the label of  $\mathbf{x}$ 
9:     Add  $(\mathbf{x}, \tilde{\mathbf{y}})$  to  $\mathcal{B}$  with time stamp of receiving  $\mathbf{x}$ 
10:  end for
11:   $\mathcal{I}_n \leftarrow$  Select a subset of model parameter indices  $\triangleright$  Entering Training Phase
12:  for  $k \in \{1, 2, \dots, K\}$  do
13:     $\mathbf{S}_k \leftarrow$  Uniformly sample a mini-batch of data points from  $\mathcal{B}$  over the last  $\tau'$  seconds
14:    Candidate updates  $\leftarrow$  Calculate Adam optimizer updates w.r.t the empirical loss on  $\mathbf{S}_k$ 
15:    Apply candidate updates to model parameters indexed by  $\mathcal{I}_n$ 
16:  end for
17:   $\tilde{\mathbf{w}}_n \leftarrow$  New value of model parameters which are indexed by  $\mathcal{I}_n$ 
18:  Send  $(\tilde{\mathbf{w}}_n, \mathcal{I}_n)$  for the edge device
19: end for

```

---

#### 4.1 Practical Challenges

**Reducing Downlink Bandwidth Requirements.** Naïvely streaming a large model to the edge device can consume a significant amount of bandwidth. For example, sending a relatively simple model with 2 million parameters every 10 seconds would require 3.2 Mbps of downlink bandwidth. In our experiments, using coordinate descent with a Gradient-Guided strategy to send 5% of the parameters in each model update reduces the required bandwidth by  $14\times$  with negligible loss in performance compared to updating the complete model. Along with the updated parameters,  $\tilde{\mathbf{w}}_n$ , we must also send their location in the model,  $\mathcal{I}_n$ , which introduces additional bandwidth overhead. A simple strategy is to send a bit-vector identifying the location of the parameters with each model update. As the bit-vector is sparse, it can be compressed and we use gzip [61] in our experiments to

carry this out. Further bandwidth reductions could be achieved using standard model compression and quantization techniques [33, 34, 36].

**Reducing Uplink Bandwidth Requirements.** To reduce the uplink bandwidth, the edge device does not send sampled frames immediately. Instead it buffers samples corresponding to  $\tau$  seconds of video (e.g.,  $\tau = 10$ ), and it runs H.264 [29] video encoding on this buffer to compress it before transmission. The time taken at the edge device to fill the compression buffer and transmit a new batch of samples is hidden from the server by overlapping it with the training phase of the previous step. By synchronizing the transmission of new data with the start of the inference phase, we minimize the staleness of the training data at the server.

**Maximizing Server Utilization.** Running a GPU in the cloud, e.g., NVIDIA Tesla V100, currently costs at least \$1 per hour. Hence, it is important to serve multiple edge devices per GPU to keep per-user cost low. Every user that joins a cloud server requires its own share of GPU resources for inference and training operations. In our prototype, we use a simple strategy that iterates in a round-robin fashion across multiple video sessions, completing one inference and training step per session. By allowing only one process to access the GPU at a time, we minimize context switching overhead. Our results show that this technique is effective and can support model streaming for up to seven video sessions per an NVIDIA Tesla V100 GPU with negligible loss in performance.

## 5 Evaluation

### 5.1 Methodology

We evaluate AMS on the task of semantic segmentation using the DeeplabV3 [2] class of models. These models have a wide range of sizes but share the same architectural ideas. As the initial model, we start with models pre-trained on the Cityscapes [16] semantic segmentation dataset. These models themselves include a backbone pre-trained on Imagenet and MS-COCO [62, 63]. On the edge device, we use the model with MobileNetV2 [11] backbone at an input image resolution of  $512 \times 256$ , which runs smoothly in real-time at 30 frame-per-second (fps) on a Samsung Galaxy S10+ phone’s Adreno 640 GPU with less than 40 ms camera-to-label latency. We compare the following schemes:

- **No Customization:** We run the pre-trained model without video-specific customization.
- **One-Time Customization:** We collect training samples at four frames per second during the first 60 seconds of the video, fine-tune the entire model on these samples at the server and send it to the edge. This adaptation happens only once for every video. Comparing this scheme with AMS will show the benefit of continuous adaptation.
- **AMS:** We use Algorithm 1 at the server with  $\tau = 10$  sec,  $\tau' = 250$  sec, and  $K = 20$  iterations. Unless otherwise stated, 5% of the model parameters are selected using the Gradient-Guided strategy. We use a single NVIDIA Tesla V100 GPU for both training and inference at the server.

One-Time Customization and AMS use DeeplabV3 with Xception65 [14] backbone pre-trained on Cityscapes as the teacher model. In both schemes, edge devices transmit sample frames at a resolution of  $1024 \times 512$  to the cloud server after compression, as described in §4.1. The server upscales the received frames to a resolution of  $1800 \times 900$  before labeling them with the teacher. For all training purposes, we use Adam optimizer [60] with a learning rate of 0.001,  $\beta_1 = 0.9$ ,  $\beta_2 = 0.999$ .

**Videos.** We use 7 diverse videos chosen from YouTube with a length of 7–15 minutes for evaluation. Since our semantic segmentation models were trained on Cityscapes driving scenes, we consider videos of outdoor scenes for which our best model with Xception65 backbone has good visual performance. However, the videos cover a range of scene variability, representing different scenarios of interest including fixed cameras and moving cameras at walking, running, and driving speeds. Table 4 and Fig. 5 in Appendix A provide a description of the videos and some examples of scenes.

**Metric.** To evaluate the accuracy of different schemes, we collect the inferred labels on the edge device and compare them against labels extracted for the same video frames using a state-of-the-art DeeplabV3 with Xception65 backbone model (pre-trained on Cityscapes) running at full resolution ( $2048 \times 1024$ ) offline. We report the mean Intersection-over-Union (mIoU) metric relative to the labels produced by this reference model. The metric computes the Intersection-over-Union (defined as the number of true positives divided by the sum of true positives, false negatives and false positives)

**Table 1:** Comparison of mIoU (in percent) for different methods across 7 evaluation videos.

	Vid1	Vid2	Vid3	Vid4	Vid5	Vid6	Vid7
No Customization	71.91	54.48	72.80	69.93	49.04	66.26	61.31
One-Time Customization	88.45	55.99	83.55	69.53	55.12	65.07	58.12
AMS (5% of parameters)	88.55	71.45	85.36	75.53	59.49	71.40	69.44

**Table 2:** AMS bandwidth usage (in Kbps) and mIoU (in percent) for updating different fraction of model parameters using the Gradient-Guided strategy.

Fraction	BW(Kbps)	Vid1	Vid2	Vid3	Vid4	Vid5	Vid6	Vid7
100%	3302	89.49	72.97	85.90	75.83	60.24	71.15	70.69
20%	812	88.91	72.83	85.52	76.38	59.65	72.56	70.57
10%	435	88.61	72.13	85.46	76.16	60.18	71.98	70.11
5%	230	88.55	71.45	85.36	75.53	59.49	71.40	69.44
1%	51.8	84.59	68.37	84.41	73.95	57.53	69.27	68.16

for each class, and takes a mean over the classes. We manually select a subset of most populous Cityscapes output classes in each of these videos as summarized in Table 4 in Appendix A.

## 5.2 Results

**Comparison to baselines.** Table 1 summarizes the results. The No Customization model has the worst accuracy among these three methods which is 5.1–17.0% (10.8% on average) below AMS. The One-Time Customization model performs better as it is specialized for each video using the initial frames. However, since a video itself can vary significantly over time, AMS performs even better by continually adapting the model to the video. AMS outperforms One-Time Customization by 0.1–15.5% (6.5% on average) across the 7 videos. It achieves the highest improvement in Vid2 due to its high scene variability (comedian performing, crowd watching, streets, etc.), which makes continuous adaptation crucial. The smallest improvement is in Vid1, a stationary interview scene, for which One-Time Customization performs well.

**Accuracy vs. bandwidth usage.** Table 2 shows the accuracy and downlink bandwidth usage for sending different fractions of the student model to the device on each update. We observe that coordinate descent is very effective. Sending only 5% of the model parameters results in only 0.76% loss of accuracy on average across the 7 videos, but it reduces the downlink bandwidth requirement significantly, from 3.3 Mbps to update the full model ( $\sim 2$  million parameters) to 230 Kbps. In the uplink, our method of compressing the sampled frames before sending to the cloud server (§4.1) requires a modest bandwidth of 100–400 Kbps (on different videos). The loss in accuracy caused by this compression is negligible (0.07% on average across the videos).

**Supporting multiple clients with one server.** In Fig. 3 we show the decrease (w.r.t. single client) in average mIoU when different number of clients share a GPU in round-robin manner. We observe that even with this simple scheduling algorithm, AMS scales to up to 7 clients on a single V100 GPU with less than 1% loss in mIoU. As we see later in the results, there is room for supporting even more clients per GPU by prioritizing certain videos that need more frequent model updates over others.

## 5.3 Impact of Design Choices

**Coordinate Descent Strategy.** Table 3 compares the Gradient-Guided strategy with four baselines for subset parameters selection in the training phase. In the *First*, *Last*, and *First&Last* strategies, the subset parameters are from the initial layers, final layers, and an equal split of both, respectively. The *Random* strategy samples parameters uniformly from the entire network. We compare these strategies on their reduction in accuracy relative to sending full model updates. We observe that the Gradient-Guided performs best, followed by Random. Random is notably worse than Gradient-Guided when training a very small fraction (1%) of model parameters. The methods that update only the first or last model layers are substantially worse than the other approaches.

**Training Horizon.** As explained using the simple example in §3, the ideal training horizon,  $\tau'$ , depends on the model capacity, with smaller models expected to perform better when trained on



**Table 3:** Difference in accuracy relative to full-model training (in percent) averaged over the 7 evaluation videos for different coordinate descent strategies.

Fraction	Gradient-Guided	Last	First	First&Last	Random
20%	+0.14	-5.43	-2.34	-0.82	-0.03
10%	-0.26	-6.13	-4.89	-1.96	-0.44
5%	-0.76	-7.95	-7.16	-2.64	-1.21
1%	-2.49	-9.97	-14.44	-6.61	-4.39

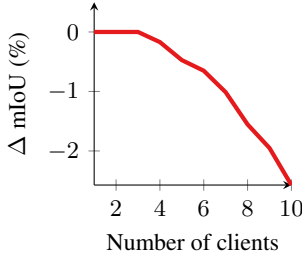


**Figure 3:** Average multicient mIoU degradation compared to single-client performance.

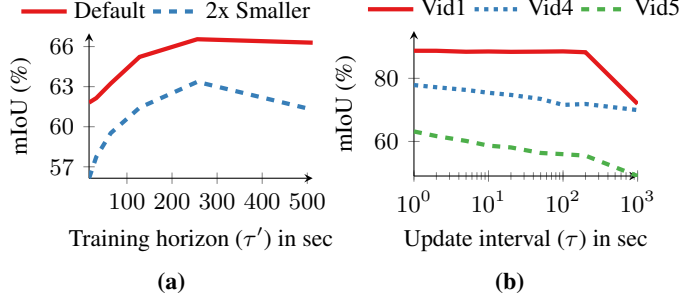


**Figure 4:** Impact of training horizon and training frequency on AMS Semantic Segmentation task.

shorter time horizons. We evaluate this intuition for the video semantic segmentation task. We consider two variations of the student model: (i) the default DeeplabV3 with MobileNetV2 backbone, (ii) a smaller version with the same architecture but with half the number of channels in each convolutional layer. We pick 50 points in time uniformly distributed over the course of one video (Vid6). For each time  $t$ , we train the two student models on the frames in the interval  $[t - \tau', t]$  and then evaluate them on frames in  $[t, t + \tau]$  (with  $\tau = 16$  sec). We plot the average accuracy of the two variants for each value of the training horizon  $\tau'$  in Fig. 4a. As expected, the smaller model’s accuracy peaks at some training horizon ( $\tau' \approx 250$  sec) and degrades with larger  $\tau'$  as the model capacity is insufficient to learn wider variations in the training data. The default student model exhibits the same behavior, but with a more gradual drop for large  $\tau'$ . Overall we found that a training horizon of 200–400 seconds generally works well across all of the videos in our dataset.

**Model Update Frequency.** The frequency of model updates dictates how long a particular model is used at the edge device. Intuitively, more frequent updates should lead to better accuracy, at the cost of higher bandwidth and server computation. To evaluate the impact of model update frequency, we measure the accuracy for three videos, with different update intervals  $\tau$  ranging from 1 to 1000 seconds and a training horizon  $\tau'$  of 256 seconds. Figure 4b shows the results. As expected, a smaller  $\tau$  improves performance, but the impact of slower model updates varies across the three videos. For example, rapid model updates barely improve Vid1, which is an interview with a stationary scene. However, the effect is visible for Vid4 and Vid5 as they are walking scenes. This suggests that we can support more video sessions per GPU by prioritizing videos that need more frequent model updates.

**Frame Sampling Rate.** Table 5 in Appendix D shows the impact of varying the frame sampling rate on accuracy for 3 videos. Sampling faster than 1 frame-per-second provides negligible improvement in accuracy along increasing bandwidth usage. As these results suggest, the sampling rate can be reduced at the cost of a small reduction in accuracy.

## 6 Conclusion

We presented an approach for improving the performance of real-time video inference on low-powered edge devices that uses a remote server to continually train and stream model updates to the edge device at a time scale of 10–100 seconds. Further, we proposed techniques to reduce the network bandwidth requirements of adaptive model streaming to levels easily sustainable on today’s wireless networks. Extensive evaluation of AMS on a wide range of videos showed a rise of 5.1–17.0% in mIoU scores on the task of real-time semantic segmentation using a mobile GPU, which can be a significant improvement for the quality of real-time video inference on edge devices.



## Broader Impact

Real-time video inference on edge devices, which our work aims to make practical, has a wide range of societal applications. Examples include tasks like semantic segmentation in autonomous driving, visual tracking and object recognition in drone navigation, infrastructure monitoring using drones, super-resolution in video streaming, object detection on home devices like robotic vacuums, and future research on enabling augmented reality with neural networks. Real-time video inference also has potential negative applications, such as privacy-violating surveillance, and real-time “deepfake” models used to impersonate others on video calls. Failure of the system can result in poor inference accuracy, with consequences that depend on the application. Like systems that rely on remote inference, our system is vulnerable to abuse by a malicious and untrusted server, since clients must stream video to a remote server for training.

## References

- [1] Joseph Redmon, Santosh Divvala, Ross Girshick, and Ali Farhadi. You only look once: Unified, real-time object detection. In *Proceedings of the IEEE conference on computer vision and pattern recognition*, pages 779–788, 2016.
- [2] Liang-Chieh Chen, George Papandreou, Iasonas Kokkinos, Kevin Murphy, and Alan L. Yuille. Deeplab: Semantic image segmentation with deep convolutional nets, atrous convolution, and fully connected crfs. *IEEE Transactions on Pattern Analysis and Machine Intelligence*, 40: 834–848, 2018.
- [3] Zhe Cao, Tomas Simon, Shih-En Wei, and Yaser Sheikh. Realtime multi-person 2d pose estimation using part affinity fields. In *Proceedings of the IEEE Conference on Computer Vision and Pattern Recognition*, pages 7291–7299, 2017.
- [4] Tensorflow. Deeplab semantic segmentation model zoo. [https://github.com/tensorflow/models/blob/master/research/deeplab/g3doc/model\\_zoo.md](https://github.com/tensorflow/models/blob/master/research/deeplab/g3doc/model_zoo.md), 2020.
- [5] Tensorflow. Tensorflow object detection model zoo. [https://github.com/tensorflow/models/blob/master/research/object\\_detection/g3doc/detection\\_model\\_zoo.md](https://github.com/tensorflow/models/blob/master/research/object_detection/g3doc/detection_model_zoo.md), 2020.
- [6] Coral Edge TPU datasheet. <https://coral.ai/docs/dev-board/datasheet/>, 2020.
- [7] NVIDIA Jetson Nano datasheet. <https://developer.nvidia.com/embedded/jetson-nano>, 2020.
- [8] Edge TPU performance benchmarks. <https://coral.ai/docs/edgetpu/benchmarks/>, 2020.
- [9] Junjue Wang, Ziqiang Feng, Zhuo Chen, Shilpa George, Mihir Bala, Padmanabhan Pillai, Shao-Wen Yang, and Mahadev Satyanarayanan. Bandwidth-efficient live video analytics for drones via edge computing. pages 159–173, 10 2018. doi: 10.1109/SEC.2018.00019.
- [10] Qianlin Liang, Prashant J. Shenoy, and David Irwin. AI on the Edge: Rethinking AI-based IoT Applications Using Specialized Edge Architectures. *ArXiv*, abs/2003.12488, 2020.
- [11] Mark Sandler, Andrew G. Howard, Menglong Zhu, Andrey Zhmoginov, and Liang-Chieh Chen. Mobilenetv2: Inverted residuals and linear bottlenecks. *2018 IEEE/CVF Conference on Computer Vision and Pattern Recognition*, pages 4510–4520, 2018.
- [12] Andrew Howard, Mark Sandler, Grace Chu, Liang-Chieh Chen, Bo Chen, Mingxing Tan, Weijun Wang, Yukun Zhu, Ruoming Pang, Vijay Vasudevan, Quoc V. Le, and Hartwig Adam. Searching for mobilenetv3. *2019 IEEE/CVF International Conference on Computer Vision (ICCV)*, pages 1314–1324, 2019.
- [13] M. Tan, B. Chen, R. Pang, V. Vasudevan, M. Sandler, A. Howard, and Q. V. Le. Mnasnet: Platform-aware neural architecture search for mobile. In *2019 IEEE/CVF Conference on Computer Vision and Pattern Recognition (CVPR)*, pages 2815–2823, 2019.

- [14] F. Chollet. Xception: Deep learning with depthwise separable convolutions. In *2017 IEEE Conference on Computer Vision and Pattern Recognition (CVPR)*, pages 1800–1807, 2017.
- [15] Mark Everingham, S. Eslami, Luc Van Gool, Christopher Williams, John Winn, and Andrew Zisserman. The pascal visual object classes challenge: A retrospective. *International Journal of Computer Vision*, 111, 01 2014. doi: 10.1007/s11263-014-0733-5.
- [16] Marius Cordts, Mohamed Omran, Sebastian Ramos, Timo Rehfeld, Markus Enzweiler, Rodrigo Benenson, Uwe Franke, Stefan Roth, and Bernt Schiele. The cityscapes dataset for semantic urban scene understanding. *2016 IEEE Conference on Computer Vision and Pattern Recognition (CVPR)*, pages 3213–3223, 2016.
- [17] Xianzhi Du, Tsung-Yi Lin, Pengchong Jin, Golnaz Ghiasi, Mingxing Tan, Yin Cui, Quoc V Le, and Xiaodan Song. Spinenet: Learning scale-permuted backbone for recognition and localization. *arXiv preprint arXiv:1912.05027*, 2019.
- [18] Christopher Olston, Noah Fiedel, Kiril Gorovoy, Jeremiah Harmsen, Li Lao, Fangwei Li, Vinu Rajashekhar, Sukriti Ramesh, and Jordan Soyke. Tensorflow-serving: Flexible, high-performance ml serving. *arXiv preprint arXiv:1712.06139*, 2017.
- [19] Daniel Crankshaw, Xin Wang, Guilio Zhou, Michael J Franklin, Joseph E Gonzalez, and Ion Stoica. Clipper: A low-latency online prediction serving system. In *14th {USENIX} Symposium on Networked Systems Design and Implementation ({NSDI} 17)*, pages 613–627, 2017.
- [20] Chengliang Zhang, Minchen Yu, Wei Wang, and Feng Yan. Mark: Exploiting cloud services for cost-effective, slo-aware machine learning inference serving. In *2019 {USENIX} Annual Technical Conference ({USENIX} {ATC} 19)*, pages 1049–1062, 2019.
- [21] Sadjad Fouladi, John Emmons, Emre Orbay, Catherine Wu, Riad S Wahby, and Keith Winstein. Salsify: Low-latency network video through tighter integration between a video codec and a transport protocol. In *15th {USENIX} Symposium on Networked Systems Design and Implementation ({NSDI} 18)*, pages 267–282, 2018.
- [22] Keith Winstein, Anirudh Sivaraman, and Hari Balakrishnan. Stochastic forecasts achieve high throughput and low delay over cellular networks. In *Presented as part of the 10th {USENIX} Symposium on Networked Systems Design and Implementation ({NSDI} 13)*, pages 459–471, 2013.
- [23] W. Shi, J. Cao, Q. Zhang, Y. Li, and L. Xu. Edge computing: Vision and challenges. *IEEE Internet of Things Journal*, 3(5):637–646, 2016.
- [24] Pedro Garcia Lopez, Alberto Montresor, Dick Epema, Anwitaman Datta, Teruo Higashino, Adriana Iamnitchi, Marinho Barcellos, Pascal Felber, and Etienne Riviere. Edge-centric computing: Vision and challenges. *SIGCOMM Comput. Commun. Rev.*, 45(5):37–42, September 2015. ISSN 0146-4833. doi: 10.1145/2831347.2831354. URL <https://doi.org/10.1145/2831347.2831354>.
- [25] Flavio Bonomi, Rodolfo Milito, Jiang Zhu, and Sateesh Addepalli. Fog computing and its role in the internet of things. In *Proceedings of the First Edition of the MCC Workshop on Mobile Cloud Computing, MCC ’12*, page 13–16, New York, NY, USA, 2012. Association for Computing Machinery. ISBN 9781450315197. doi: 10.1145/2342509.2342513. URL <https://doi.org/10.1145/2342509.2342513>.
- [26] Geoffrey Hinton, Oriol Vinyals, and Jeff Dean. Distilling the knowledge in a neural network. *arXiv preprint arXiv:1503.02531*, 2015.
- [27] Stephen J. Wright. Coordinate descent algorithms. *Mathematical Programming*, 151:3–34, 2015.
- [28] Yurii NESTEROV. Efficiency of coordinate descent methods on huge-scale optimization problems. *Université catholique de Louvain, Center for Operations Research and Econometrics (CORE), CORE Discussion Papers*, 22, 01 2010. doi: 10.1137/100802001.

- [29] T. Wiegand, G. J. Sullivan, G. Bjontegaard, and A. Luthra. Overview of the h.264/avc video coding standard. *IEEE Transactions on Circuits and Systems for Video Technology*, 13(7): 560–576, 2003.
- [30] Choose live encoder settings, bitrates, and resolutions. <https://support.google.com/youtube/answer/2853702?hl=en>. Accessed: 2020-06-01.
- [31] Barret Zoph and Quoc V Le. Neural architecture search with reinforcement learning. *arXiv preprint arXiv:1611.01578*, 2016.
- [32] Bichen Wu, Xiaoliang Dai, Peizhao Zhang, Yanghan Wang, Fei Sun, Yiming Wu, Yuandong Tian, Peter Vajda, Yangqing Jia, and Kurt Keutzer. Fbnet: Hardware-aware efficient convnet design via differentiable neural architecture search. In *Proceedings of the IEEE Conference on Computer Vision and Pattern Recognition*, pages 10734–10742, 2019.
- [33] Yihui He, Ji Lin, Zhijian Liu, Hanrui Wang, Li-Jia Li, and Song Han. Amc: Automl for model compression and acceleration on mobile devices. In *Proceedings of the European Conference on Computer Vision (ECCV)*, pages 784–800, 2018.
- [34] Darryl Lin, Sachin Talathi, and Sreekanth Annapureddy. Fixed point quantization of deep convolutional networks. In *International Conference on Machine Learning*, pages 2849–2858, 2016.
- [35] Davis Blalock, Jose Javier Gonzalez Ortiz, Jonathan Frankle, and John Gutttag. What is the state of neural network pruning? *arXiv preprint arXiv:2003.03033*, 2020.
- [36] Yu Cheng, Duo Wang, Pan Zhou, and Tao Zhang. A survey of model compression and acceleration for deep neural networks. *ArXiv*, abs/1710.09282, 2017.
- [37] Zheng Zhu, Qiang Wang, Bo Li, Wei Wu, Junjie Yan, and Weiming Hu. Distractor-aware siamese networks for visual object tracking. In *Proceedings of the European Conference on Computer Vision (ECCV)*, pages 101–117, 2018.
- [38] Xizhou Zhu, Yuwen Xiong, Jifeng Dai, Lu Yuan, and Yichen Wei. Deep feature flow for video recognition. In *Proceedings of the IEEE Conference on Computer Vision and Pattern Recognition*, pages 2349–2358, 2017.
- [39] Yuan-Ting Hu, Jia-Bin Huang, and Alexander Schwing. Maskrnn: Instance level video object segmentation. In *Advances in neural information processing systems*, pages 325–334, 2017.
- [40] Yiping Kang, Johann Hauswald, Cao Gao, Austin Rovinski, Trevor Mudge, Jason Mars, and Lingjia Tang. Neurosurgeon: Collaborative intelligence between the cloud and mobile edge. *ACM SIGARCH Computer Architecture News*, 45(1):615–629, 2017.
- [41] Sandeep P Chinchali, Eyal Cidon, Evgenya Pergament, Tianshu Chu, and Sachin Katti. Neural networks meet physical networks: Distributed inference between edge devices and the cloud. In *Proceedings of the 17th ACM Workshop on Hot Topics in Networks*, pages 50–56, 2018.
- [42] Sandeep Chinchali, Apoorva Sharma, James Harrison, Amine Elhafsi, Daniel Kang, Evgenya Pergament, Eyal Cidon, Sachin Katti, and Marco Pavone. Network offloading policies for cloud robotics: a learning-based approach. *arXiv preprint arXiv:1902.05703*, 2019.
- [43] Shai Shalev-Shwartz et al. Online learning and online convex optimization. *Foundations and Trends® in Machine Learning*, 4(2):107–194, 2012.
- [44] Eric C Hall and Rebecca M Willett. Dynamical models and tracking regret in online convex programming. In *Proceedings of the 30th International Conference on International Conference on Machine Learning-Volume 28*, pages I–579, 2013.
- [45] Lijun Zhang, Shiyin Lu, and Zhi-Hua Zhou. Adaptive online learning in dynamic environments. In *Advances in neural information processing systems*, pages 1323–1333, 2018.
- [46] Aryan Mokhtari, Shahin Shahrampour, Ali Jadbabaie, and Alejandro Ribeiro. Online optimization in dynamic environments: Improved regret rates for strongly convex problems. In *2016 IEEE 55th Conference on Decision and Control (CDC)*, pages 7195–7201. IEEE, 2016.

- [47] Martin Zinkevich. Online convex programming and generalized infinitesimal gradient ascent. In *Proceedings of the 20th international conference on machine learning (icml-03)*, pages 928–936, 2003.
- [48] Elad Hazan, Amit Agarwal, and Satyen Kale. Logarithmic regret algorithms for online convex optimization. *Machine Learning*, 69(2-3):169–192, 2007.
- [49] Mark Herbster and Manfred K Warmuth. Tracking the best expert. *Machine learning*, 32(2): 151–178, 1998.
- [50] Tianbao Yang, Lijun Zhang, Rong Jin, and Jinfeng Yi. Tracking slowly moving clairvoyant: optimal dynamic regret of online learning with true and noisy gradient. In *Proceedings of the 33rd International Conference on International Conference on Machine Learning-Volume 48*, pages 449–457, 2016.
- [51] Elad Hazan and Comandur Seshadhri. Efficient learning algorithms for changing environments. In *Proceedings of the 26th annual international conference on machine learning*, pages 393–400, 2009.
- [52] David Lopez-Paz and Marc’Aurelio Ranzato. Gradient episodic memory for continual learning. In *Advances in Neural Information Processing Systems*, pages 6467–6476, 2017.
- [53] Chelsea Finn, Pieter Abbeel, and Sergey Levine. Model-agnostic meta-learning for fast adaptation of deep networks. In *Proceedings of the 34th International Conference on Machine Learning-Volume 70*, pages 1126–1135. JMLR. org, 2017.
- [54] Sachin Ravi and Hugo Larochelle. Optimization as a model for few-shot learning. *International Conference on Learning Representations (ICLR)*, 2017.
- [55] Brendan McMahan, Eider Moore, Daniel Ramage, Seth Hampson, and Blaise Aguerre y Arcas. Communication-efficient learning of deep networks from decentralized data. In *Artificial Intelligence and Statistics*, pages 1273–1282, 2017.
- [56] Shai Ben-David, John Blitzer, Koby Crammer, and Fernando Pereira. Analysis of representations for domain adaptation. In *Advances in neural information processing systems*, pages 137–144, 2007.
- [57] Guoliang Kang, Lu Jiang, Yi Yang, and Alexander G Hauptmann. Contrastive adaptation network for unsupervised domain adaptation. In *Proceedings of the IEEE Conference on Computer Vision and Pattern Recognition*, pages 4893–4902, 2019.
- [58] Daniel Kang, John Emmons, Firas Abuzaid, Peter Bailis, and Matei Zaharia. Noscope: optimizing neural network queries over video at scale. *arXiv preprint arXiv:1703.02529*, 2017.
- [59] Ravi Teja Mullapudi, Steven Chen, Keyi Zhang, Deva Ramanan, and Kayvon Fatahalian. Online model distillation for efficient video inference. In *Proceedings of the IEEE International Conference on Computer Vision*, pages 3573–3582, 2019.
- [60] Diederik P. Kingma and Jimmy Ba. Adam: A method for stochastic optimization. *CoRR*, abs/1412.6980, 2015.
- [61] P. Deutsch. Rfc1952: Gzip file format specification version 4.3, 1996.
- [62] J. Deng, W. Dong, R. Socher, L. Li, Kai Li, and Li Fei-Fei. Imagenet: A large-scale hierarchical image database. In *2009 IEEE Conference on Computer Vision and Pattern Recognition*, pages 248–255, 2009.
- [63] Tsung-Yi Lin, Michael Maire, Serge J. Belongie, James Hays, Pietro Perona, Deva Ramanan, Piotr Dollár, and C. Lawrence Zitnick. Microsoft coco: Common objects in context. *ArXiv*, abs/1405.0312, 2014.
- [64] David Rolnick, Arun Ahuja, Jonathan Schwarz, Timothy Lillicrap, and Gregory Wayne. Experience replay for continual learning. In *Advances in Neural Information Processing Systems*, pages 348–358, 2019.

- [65] James Kirkpatrick, Razvan Pascanu, Neil Rabinowitz, Joel Veness, Guillaume Desjardins, Andrei A Rusu, Kieran Milan, John Quan, Tiago Ramalho, Agnieszka Grabska-Barwinska, et al. Overcoming catastrophic forgetting in neural networks. *Proceedings of the national academy of sciences*, 114(13):3521–3526, 2017.
- [66] Michael McCloskey and Neal J Cohen. Catastrophic interference in connectionist networks: The sequential learning problem. In *Psychology of learning and motivation*, volume 24, pages 109–165. Elsevier, 1989.
- [67] Chelsea Finn, Aravind Rajeswaran, Sham Kakade, and Sergey Levine. Online meta-learning. *arXiv preprint arXiv:1902.08438*, 2019.
- [68] Keith Bonawitz, Hubert Eichner, Wolfgang Grieskamp, Dzmitry Huba, Alex Ingerman, Vladimir Ivanov, Chloe Kiddon, Jakub Konecny, Stefano Mazzocchi, H Brendan McMahan, et al. Towards federated learning at scale: System design. *arXiv preprint arXiv:1902.01046*, 2019.
- [69] Julie Nutini, Mark Schmidt, Issam H. Laradji, Michael Friedlander, and Hoyt Koepke. Co-ordinate descent converges faster with the gauss-southwell rule than random selection. In *Proceedings of the 32nd International Conference on International Conference on Machine Learning - Volume 37*, ICML’15, page 1632–1641. JMLR.org, 2015.

## Appendix A Videos

Our video corpus includes seven publicly available videos from Youtube, with 7–15 minutes in duration. These videos span different levels of scene variability and were captured with four types of cameras: Stationary, Phone, Headcam, and DashCam. For each video, we manually select 5–7 classes that are detected frequently by our best semantic segmentation model (DeeplabV3 with Xception65 backbone trained on Cityscapes data) at full resolution. Table 4 shows summary information about these videos. In Fig. 5 we show six sample frames for each video. For viewing the raw and labeled videos, please refer to <https://github.com/modelstreaming/ams>.

**Table 4:** Videos description

Tag	Description	Camera Style	Classes
Vid1	Interview with head-coach	Stationary	Buildings, Vegetation, Terrain, Sky, People, Cars
Vid2	Street comedian in Rome	Phone	Streets, Sidewalks, Buildings, Vegetation, Sky, People
Vid3	Group dance in a park	Stationary	Sidewalks, Buildings, Vegetation, Sky, People
Vid4	Street walking in Paris	Phone	Streets, Buildings, Vegetation, Sky, People, Cars
Vid5	Street walking in NYC	Phone	Streets, Buildings, Vegetation, Sky, People, Cars
Vid6	Driving in LA	4K DashCam	Streets, Sidewalks, Buildings, Vegetation, Sky, People, Cars
Vid7	Bubble run in Honolulu	Headcam	Streets, Terrain, Vegetation, Sky, Person

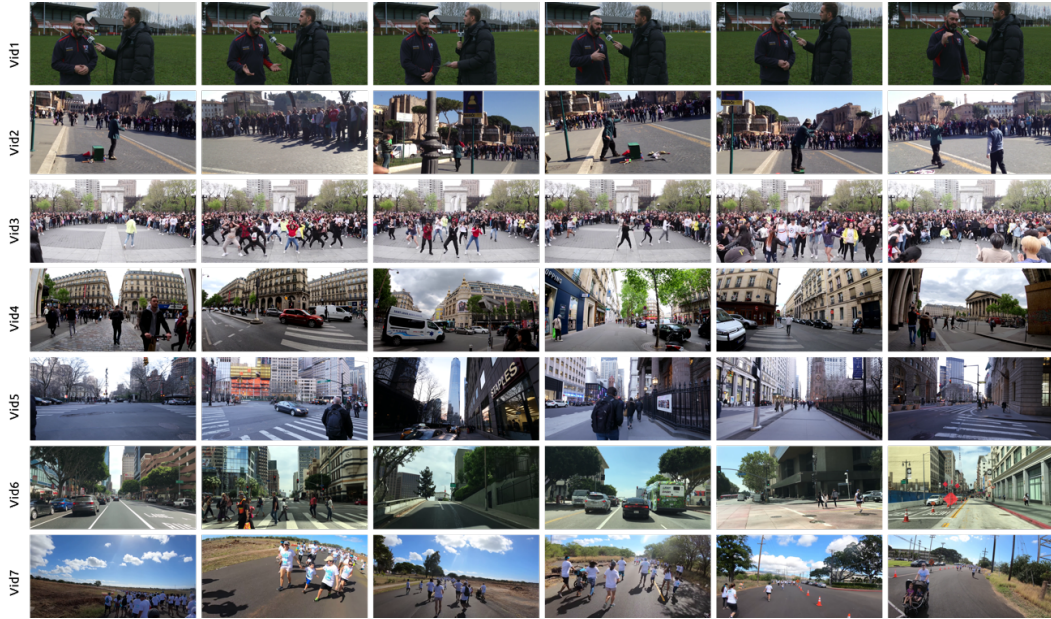


**Figure 5:** Sample video frames.

## Appendix B Other Related Work

**Continual/Lifelong Learning.** The goal of lifelong learning [52] is to accumulate knowledge over time [64]. Hence the main challenge is to improve the model based on new data over time, while not forgetting data observed in the past [65, 66]. However, as the lightweight models have limited capacity, in AMS we aim to track the best model at each point in time, and these models are allowed not to have the same performance on the old data.

**Meta Learning.** Meta learning [53, 54, 67] algorithms aim to learn models that can be adapted to any target task in a set of tasks, given only few samples (shots) from that task. Meta learning is not a natural framework for continual model specialization for video. First, as videos have temporal



coherence, there is little benefit in handling an arbitrary order of task arrival. Indeed, it is more natural to adapt the latest model over time instead of always training from a meta-learned initial model.<sup>1</sup> Second, training such a meta model usually requires two nested optimization steps [53], which would significantly increase the server’s computation overhead. Finally, most meta learning work considers a finite set of tasks but this notion is not well-suited to video.

**Federated Learning.** Another body of work on improving edge models over time is federated learning [55], in which the training mainly happens on the edge devices and device updates are aggregated at a server. The server then broadcasts the aggregated model back to all devices. Such updates happen at a time scale of hours to days [68], and they aim to learn better generalizable models that incorporate data from all edge devices. In contrast, the training in AMS takes place at the server at a time scale of a couple of seconds and intends to improve the accuracy of an individual edge device’s model for its particular video.

**Unsupervised Adaptation.** Domain adaptation methods [56, 57] intend to compensate for shifts between training and test data distributions. In a typical approach, an unsupervised algorithm fine-tunes the model over the entire test data at once. However, frame distribution can drift over time. As our results show, one-time fine-tuning can have a much lower accuracy than continuous adaptation. However, it is too expensive to provide a fast adaptation (at a timescale of 10–100 seconds) of these models at the edge, even using unsupervised methods. Moreover, using AMS we benefit from the superior performance of supervised training by running state-of-the-art models as the “teacher” for knowledge distillation [26] in the cloud.

## Appendix C The *Gradient-Guided* strategy

To reduce the bandwidth requirement of model streaming, we employ coordinate descent [27] training. In each training phase, we select a small subset (e.g., 5%) of parameters (coordinates) to update. We expand the Lines 11–16 in Algorithm 1 by adding the details of Gradient-Guided strategy as in Algorithm 2.

The pseudo code describes the procedure in the  $n^{th}$  training phase. Each training phase includes  $K$  iterations with randomly-sampled mini-batches of data points from the last  $\tau'$  seconds of video. In training iteration  $k$ , we update the first and second moments of the optimizer ( $\mathbf{m}_{n,k}$  and  $\mathbf{v}_{n,k}$ ) using the typical Adam rules (Lines 7–10). We then calculate the Adam updates for all model parameters  $\mathbf{u}_{n,k}$  (Lines 11–12). However, we only apply the updates for parameters determined by the binary mask  $\mathbf{b}_n$  (Line 13). Here,  $\mathbf{b}_n$  is a vector of the same size as the model parameters, with ones at indices that are in  $\mathcal{I}_n$  and zeros otherwise. In the Gradient-Guided strategy, we select the  $\mathcal{I}_n$  to index the  $\gamma$  fraction of parameters with the largest absolute value of the vector  $\mathbf{u}_{n-1}$ . We update  $\mathbf{u}_n$  at the end of each training phase to reflect the latest values of the Adam updates for all parameters (Line 15). In the first training phase,  $\mathcal{I}_n$  is selected uniformly at random.

The intuition behind this algorithm is to update the subset of parameters that could provide the largest improvement in the loss function. A typical way to achieve this would be to update the parameters with the largest gradient magnitude in each training phase. This is called the *Gauss-Southwell selection rule* [69]. Algorithm 2 applies this intuition to coordinate descent using the Adam optimizer [60]. To perform coordinate descent using Adam, we consider the parameters with the largest magnitude of change in Adam’s parameter update. Adam uses the first and second moments of past gradients to suggest a less noisy and more robust parameter update than just the gradient for one mini-batch. Notice, however, that to use this signal, we have to update the moments for all parameters in all training iterations, regardless of whether or not we actually update those parameters in Line 13.

## Appendix D Effect of Sampling Rate

To evaluate the effects of sampling rate, we profiled AMS’s performance for different sampling rates, ranging from one frame every 10 secs to 30 frames per second (all available frames). In this experiment, we use a training horizon of  $\tau' = 250$  seconds and a model update interval of  $\tau = 10$  seconds. To minimize the impact of other system design choices, we train the entire model parameters

<sup>1</sup>An exception is a video that changes substantially in a short period of time, for example, a camera that moves between indoor and outdoor environments. In such cases, a meta model may enable faster adaptation.



---

**Algorithm 2** *Gradient-Guided Strategy using Adam Optimizer*

---

```
1:  $\mathcal{I}_n \leftarrow$  Indices of  $\gamma$  fraction of largest absolute values in  $\mathbf{u}_{n-1}$   $\triangleright$  Entering  $n^{th}$  Training Phase
2:  $\mathbf{b}_n \leftarrow$  binary mask of model parameters; 1 iff indexed by  $\mathcal{I}_n$ 
3:  $\mathbf{w}_{n,0} \leftarrow \mathbf{w}_{n-1}$   $\triangleright$  Use the latest model parameters as the next starting point
4:  $\mathbf{m}_{n,0} \leftarrow \mathbf{m}_{n-1,K}$   $\triangleright$  Initialize the first moment estimate to its latest value
5:  $\mathbf{v}_{n,0} \leftarrow \mathbf{v}_{n-1,K}$   $\triangleright$  Initialize the second moment estimate to its latest value
6: for  $k \in \{1, 2, \dots, K\}$  do
7:    $\mathbf{S}_k \leftarrow$  Uniformly sample a mini-batch of data points from  $\mathcal{B}$  over the last  $\tau'$  seconds
8:    $\mathbf{g}_{n,k} \leftarrow \nabla_{\mathbf{w}} \tilde{\mathcal{L}}(\mathbf{S}_k; \mathbf{w}_{n,k-1})$   $\triangleright$  Get the gradient of all model parameters w.r.t. loss on  $\mathcal{S}_k$ 
9:    $\mathbf{m}_{n,k} \leftarrow \beta_1 \cdot \mathbf{m}_{n,k-1} + (1 - \beta_1) \cdot \mathbf{g}_{n,k}$   $\triangleright$  Update first moment estimate
10:   $\mathbf{v}_{n,k} \leftarrow \beta_2 \cdot \mathbf{v}_{n,k-1} + (1 - \beta_2) \cdot \mathbf{g}_{n,k}^2$   $\triangleright$  Update second moment estimate
11:   $i \leftarrow i + 1$   $\triangleright$  Increment Adam's global step count
12:   $\mathbf{u}_{n,k} \leftarrow \alpha \cdot \frac{\sqrt{1-\beta_2^i}}{1-\beta_1^i} \cdot \frac{\mathbf{m}_{n,k}}{\sqrt{\mathbf{v}_{n,k} + \epsilon}}$   $\triangleright$  Calculate the Adam updates for all model parameters
13:   $\mathbf{w}_{n,k} \leftarrow \mathbf{w}_{n,k-1} - \mathbf{u}_{n,k} * \mathbf{b}_n$   $\triangleright$  Update the parameters indexed by  $\mathcal{I}_n$  (* is elem.-wise mul.)
14: end for
15:  $\mathbf{u}_n \leftarrow \mathbf{u}_{n,K}$ 
16:  $\mathbf{w}_n \leftarrow \mathbf{w}_{n,K}$ 
```

---

in every update, starting from the pre-trained checkpoint. Table 5 shows the impact of sampling rate on mIoU across different videos. We observe that there is negligible performance improvement across all videos in sampling faster than a single frame per second.

**Table 5:** Impact of training frame sampling rate on mIoU.

Sampling Rate (fps)	30	10	3.3	1	0.33	0.1
Vid1	87.76	87.60	87.78	87.72	87.01	86.31
Vid2	71.68	71.82	71.69	71.85	71.55	70.50
Vid3	85.34	85.26	85.39	85.27	85.12	84.74
Vid4	75.22	74.21	75.29	75.07	74.21	72.71
Vid5	58.45	58.29	58.08	57.89	57.50	54.67
Vid6	71.76	71.11	71.42	71.59	69.90	69.45
Vid7	70.76	70.92	70.16	70.75	69.93	68.95